International Journal of Mechanical Engineering and Technology (IJMET)
Volume 9, Issue 1, January 2018, pp. 1022–1036 Article ID: IJMET_09_01_109
Available online at http://www.iaeme.com/IJMET/issues.asp?JType=IJMET&VType=9&IType=1
ISSN Print: 0976-6340 and ISSN Online: 0976-6359

HALL EFFECTS ON PERISTALTIC FLOW OF A COUPLE STRESS FLUID IN AN INCLINED ASYMMETRIC CHANNEL WITH PERMEABLE WALLS

J.Suresh Goud and R.Hemadri Reddy
Department of Mathematics, School of Advanced Sciences, VIT University,
Vellore, Tamil Nadu, India

ABSTRACT

In this paper we investigated the Hall Effects on peristaltic flow of a couple stress fluids in an inclined asymmetric channel with permeable walls. The study is motivated towards investigating the peristaltic mechanism in the digestive system by considering the particle size effects. Perturbation method has been used to get the solution using long wavelength approximation with low Reynolds number and dynamic boundary conditions. The effect of Hall parameter, couple stress fluid parameter, Hartmann number and permeability parameter on the pumping characteristics, temperature and concentration are discussed graphically.

Keywords: Hall Effect, Couple stress fluid, Peristaltic flow, Permeability.

Cite this Article: J.Suresh Goud and R.Hemadri Reddy, Hall effects on peristaltic flow of a couple stress fluid in an inclined asymmetric channel with permeable walls, International Journal of Mechanical Engineering and Technology 9(1), 2018. pp. 1022–1036.
http://www.iaeme.com/IJMET/issues.asp?JType=IJMET&VType=9&IType=1

1. INTRODUCTION

The word peristalsis stems from the Greek work peristalikos, which means clasping and compressing. It is used to describe a progressive wave of contraction along a channel or tube whose cross-sectional area consequently varies. In physiology, it has been found to be involved in many biological organs. In particular peristalsis may be a main mechanism for urine transport from kidney to bladder through the ureter, movement of chyme in the gastrointestinal tract, transport of lymph in the lymphatic vessels and the vasomotion of small blood vessels. In addition peristaltic pumps are designed by engineers for pumping corrosive fluids without contact with the walls of the pumping machinery.

Peristalsis mechanism has attracted the attention of many researchers' since the first investigation of fluid motion in peristaltic pump by Latham [1] and Shapiro et al. [2] in 1966. After that a number of exact, analytical, and numerical studies of peristaltic transport for Newtonian and non-Newtonian fluids have been investigated by so many researchers.

Studies pertaining to the couple stress fluid behavior are very useful, because such studies bear the potential to better explain the behavior of rheologically complex fluids, such as liquid crystals, polymeric suspensions that has have long chain molecules, lubrication as well as human sub human blood [3,4,5,6]. Valanis and Sun[7] as well as Popel et al.[8] remarked the couple stress fluids constitute a special class of non-Newtonian fluids that take account of the particle size. The couple stress theory presented by stokes [3] is quite suitable to study blood flow in micro vessels by taking the size of the erythrocytes into account. Shehawey and Mekheimer[9] analysed the flow of a couple stress fluid for any arbitrary Reynolds number and wave number considering the wave amplitude to be small.

Cowin [10], Beg et al. [11], Ali et al. [12] stressed the importance of couple stress effects in studies related to physiological and some other fluids. Some of the studies which deal with the Hall effects in peristaltic movement are done by Hayat et al. [13] in which, peristaltic flow of Maxwell fluid in the existence of Hall current. Srinivas et al. [14] studied the problem of peristaltic flow of a Newtonian fluid with heat transfer in a vertical asymmetric channel through porous medium.

Nadeem et al. [15] discussed about the influence of heat and mass transfer on the peristaltic flow of a Johnson Segalman fluid with induced magnetic field. Kavitha et al. [16] reviewed the peristaltic flow of a micropolar fluid in a vertical channel with long wavelength approximation. Vajravelu et al. [17] investigated the peristaltic flow of a Jeffrey fluid in a vertical porous stratum with heat transfer. Rami Reddy et al. [18] explored the peristaltic motion of a viscous conducting fluid through a porous medium in an asymmetric vertical channel by using Lubrication approach. Gad [19] studied the peristaltic flow of a particle-fluid in regards to Hall current. Abo-Eldahab et al [20] discussed the Hall current in peristaltic flow of viscous fluid in a vertical asymmetric channel. A.Govindarajan et al. [21] discussed the combined effect of Heat and mass transfer on MHD peristaltic flow of couple stress fluid in an inclined asymmetric channel through porous medium. J.Srinivas and J.V Ramana murthy [22] discussed flow of two immiscible couple stress fluids between two permeable beds. Hayat et al. [23] discussed the peristaltic flow of couple stress fluid in an inclined asymmetric channel. The effects of Hall current, heat and mass transfer in the presence of inclined magnetic field are also reviewed.

In this existing paper, we discussed about the Hall effects on peristaltic flow of couple stress fluid in an inclined asymmetric channel with permeable walls. The velocity, pressure gradient, temperature and concentration profiles are obtained and the results are discussed graphically.

2. MATHEMATICAL MODEL

Consider the two-dimensional peristaltic flow of couple stress fluid in an inclined asymmetric channel. The walls of the channel are separated through distance $d_1 + d_2$, the temperature maintained at the walls are T_0 and T_1 respectively. The concentration field associated to walls of the channel are taken as C_0 and C_1 respectively. The fluid is permitted by permeable walls with parameter β and magnetic field in the form $B_0 = (B_0 \sin\theta, B_0 \cos\theta, 0)$. in addition the effect due to Hall current is present.

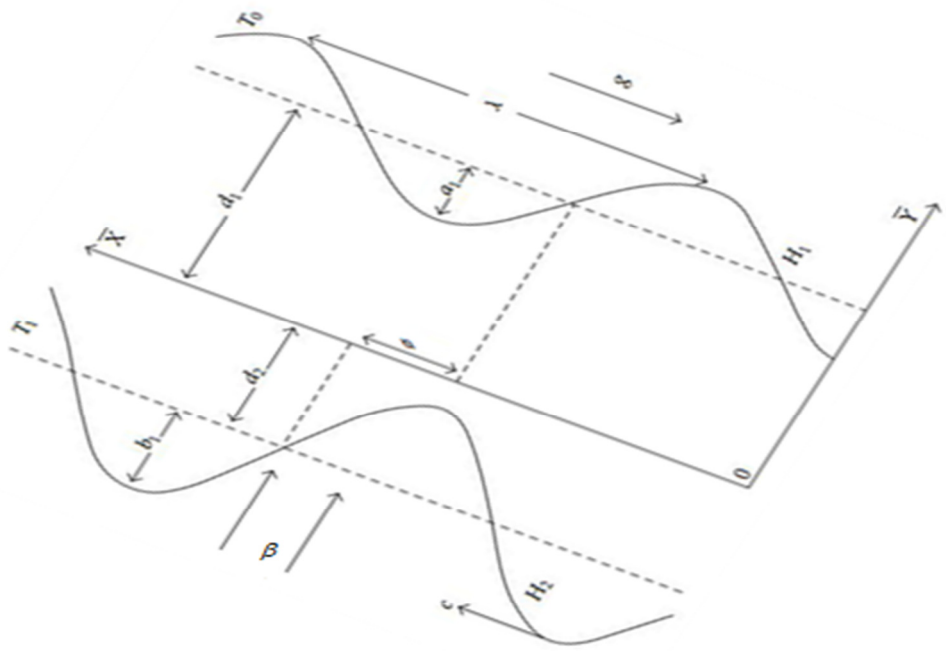

Figure 1 Physical model

The continuity, momentum, energy and concentration equation for the flow under consideration can be expressed as follows:

$$\frac{\partial \bar{U}}{\partial \bar{X}}+\frac{\partial \bar{V}}{\partial \bar{Y}}=0, \tag{1}$$

$$\rho\left(\frac{\partial}{\partial t}+\bar{U}\frac{\partial}{\partial \bar{X}}+\bar{V}\frac{\partial}{\partial \bar{Y}}\right)\bar{U}=-\frac{\partial \bar{P}}{\partial \bar{X}}+\mu\left(\frac{\partial^2 \bar{U}}{\partial \bar{X}^2}+\frac{\partial^2 \bar{U}}{\partial \bar{Y}^2}\right)-\eta^*\left(\frac{\partial^4 \bar{U}}{\partial \bar{X}^2}+2\frac{\partial^4 \bar{U}}{\partial \bar{X}^2\partial \bar{Y}^2}+\frac{\partial^4 \bar{U}}{\partial \bar{Y}^4}\right)$$
$$-\frac{\sigma^* B_0^2}{1+m^2}\cos\theta\left(\bar{U}\cos\theta-\bar{V}\sin\theta\right)+g\rho\sin\alpha \tag{2}$$

$$\rho\left(\frac{\partial}{\partial t}+\bar{U}\frac{\partial}{\partial \bar{X}}+\bar{V}\frac{\partial}{\partial \bar{Y}}\right)\bar{V}=-\frac{\partial \bar{P}}{\partial \bar{Y}}+\mu\left(\frac{\partial^2 \bar{V}}{\partial \bar{X}^2}+\frac{\partial^2 \bar{V}}{\partial \bar{Y}^2}\right)-\eta^*\left(\frac{\partial^4 \bar{V}}{\partial \bar{X}^2}+2\frac{\partial^4 \bar{V}}{\partial \bar{X}^2\partial \bar{Y}^2}+\frac{\partial^4 \bar{V}}{\partial \bar{Y}^4}\right)$$
$$-\frac{\sigma^* B_0^2}{1+m^2}\sin\theta\left(\bar{U}\cos\theta-\bar{V}\sin\theta\right)-g\rho\cos\alpha \tag{3}$$

$$\rho\xi\left(\frac{\partial}{\partial \bar{t}}+\bar{U}\frac{\partial}{\partial \bar{X}}+\bar{V}\frac{\partial}{\partial \bar{Y}}\right)T=k\left(\frac{\partial^2 T}{\partial \bar{X}^2}+\frac{\partial^2 T}{\partial \bar{Y}^2}\right)+\mu\left[2\left(\frac{\partial \bar{U}}{\partial \bar{X}}\right)^2+2\left(\frac{\partial \bar{V}}{\partial \bar{Y}}\right)^2+\left(\frac{\partial \bar{U}}{\partial \bar{Y}}+\frac{\partial \bar{V}}{\partial \bar{X}}\right)^2\right]+$$
$$\eta^*\left[\left(\frac{\partial^2 \bar{V}}{\partial \bar{X}^2}+\frac{\partial^2 \bar{V}}{\partial \bar{Y}^2}\right)^2+\left(\frac{\partial^2 \bar{U}}{\partial \bar{X}^2}+\frac{\partial^2 \bar{U}}{\partial \bar{Y}^2}\right)^2\right]+\frac{\rho D K_T}{c_s}\left(\frac{\partial^2 C}{\partial \bar{X}^2}+\frac{\partial^2 C}{\partial \bar{Y}^2}\right) \tag{4}$$

$$\left(\frac{\partial}{\partial \bar{t}}+\bar{U}\frac{\partial}{\partial \bar{X}}+\bar{V}\frac{\partial}{\partial \bar{Y}}\right)C=D\left(\frac{\partial^2 C}{\partial \bar{X}^2}+\frac{\partial^2 C}{\partial \bar{Y}^2}\right)+\frac{DK_T}{T_m}\left(\frac{\partial^2 T}{\partial \bar{X}^2}+\frac{\partial^2 T}{\partial \bar{Y}^2}\right), \tag{5}$$

The geometry of the channel walls is given by

$$\bar{Y} = \bar{h}_1 = d_1 + a_1 \sin\left[\frac{2\pi}{\lambda}\left(\bar{X} - c\bar{t}\right)\right], \tag{6}$$

$$\bar{Y} = \bar{h}_2 = -d_2 + a_2 \sin\left[\frac{2\pi}{\lambda}\left(\bar{X} - c\bar{t}\right) + \phi\right], \tag{7}$$

In Equations (1) - (7), $\bar{P}, C, T, k, \xi, T_m, D, \rho, K_T, \bar{U}, \bar{V}$ and λ are the pressure, fluid concentration, fluid temperature, thermal conductivity, specific heat at constant pressure, mean temperature of the medium, coefficient of mass diffusivity, fluid density, thermal-diffusion ratio, longitudinal velocity component, transverse velocity component and wavelength, respectively. Here, η^* is the couple stress fluid parameter, c_s is the concentration susceptibility, $a_i (i = 1,2)$ are the wave amplitudes at the upper and lower walls $\bar{t}$ is the time, ϕ is the phase difference varying in the range $0 \le \phi \le \pi$, Moreover a_i, b_i and d_i $(i = 1,2)$ satisfy the condition

$$a_1^2 + a_2^2 + 2a_1 a_2 \cos\phi \le (d_1 + d_2)^2. \tag{8}$$

Defining the transformations

$$\begin{aligned} &\bar{x} = \bar{X} - c\bar{t}, \quad \bar{y} = \bar{Y}, \quad \bar{u}(\bar{x}, \bar{y}) = \bar{U}(\bar{X}, \bar{Y}, \bar{t}), - c, \\ &\bar{v}(\bar{x}, \bar{y}) = \bar{V}(\bar{X}, \bar{Y}, \bar{t}), \quad \bar{p}(\bar{x}, \bar{y}) = \bar{P}(\bar{X}, \bar{Y}, \bar{t}), \end{aligned} \tag{9}$$

The equations in wave frame becomes

$$\frac{\partial \bar{u}}{\partial \bar{x}} + \frac{\partial \bar{v}}{\partial \bar{y}} = 0, \tag{10}$$

$$\begin{aligned} \rho\left(\bar{u}\frac{\partial}{\partial \bar{x}} + \bar{v}\frac{\partial}{\partial \bar{y}}\right)\bar{u} = &-\frac{\partial \bar{p}}{\partial \bar{x}} + \mu\left(\frac{\partial^2 \bar{u}}{\partial \bar{x}^2} + \frac{\partial^2 \bar{u}}{\partial \bar{y}^2}\right) - \eta^*\left(\frac{\partial^4 \bar{u}}{\partial \bar{x}^4} + 2\frac{\partial^4 \bar{u}}{\partial \bar{x}^2 \partial \bar{y}^2} + \frac{\partial^4 \bar{u}}{\partial \bar{y}^4}\right) \\ &- \frac{\sigma^* B_0^2}{1 + m^2}\cos\theta\left[(\bar{u} + c)\cos\theta - \bar{v}\sin\theta\right] + g\rho\sin\alpha \end{aligned} \tag{11}$$

$$\begin{aligned} \rho\left(\bar{u}\frac{\partial}{\partial \bar{x}} + \bar{v}\frac{\partial}{\partial \bar{y}}\right)\bar{v} = &-\frac{\partial \bar{p}}{\partial \bar{y}} + \mu\left(\frac{\partial^2 \bar{v}}{\partial \bar{x}^2} + \frac{\partial^2 \bar{v}}{\partial \bar{y}^2}\right) - \eta^*\left(\frac{\partial^4 \bar{v}}{\partial \bar{x}^4} + 2\frac{\partial^4 \bar{v}}{\partial \bar{x}^2 \partial \bar{y}^2} + \frac{\partial^4 \bar{v}}{\partial \bar{y}^4}\right) \\ &- \frac{\sigma^* B_0^2}{1 + m^2}\sin\theta\left[(\bar{u} + c)\cos\theta - \bar{v}\sin\theta\right] - g\rho\cos\alpha \end{aligned} \tag{12}$$

$$\begin{aligned} \rho\xi\left(\bar{u}\frac{\partial}{\partial \bar{x}} + \bar{v}\frac{\partial}{\partial \bar{y}}\right)T = &\, k\left(\frac{\partial^2 T}{\partial \bar{x}^2} + \frac{\partial^2 T}{\partial \bar{y}^2}\right) + \mu\left[2\left(\frac{\partial \bar{u}}{\partial \bar{x}}\right)^2 + 2\left(\frac{\partial \bar{u}}{\partial \bar{y}}\right)^2 + \left(\frac{\partial \bar{u}}{\partial \bar{y}} + \frac{\partial \bar{v}}{\partial \bar{x}}\right)^2\right] \\ &+ \eta^*\left[\left(\frac{\partial^2 \bar{v}}{\partial \bar{x}^2} + \frac{\partial^2 \bar{v}}{\partial \bar{y}^2}\right)^2 + \left(\frac{\partial^2 \bar{u}}{\partial \bar{x}^2} + \frac{\partial^2 \bar{u}}{\partial \bar{y}^2}\right)^2\right] + \frac{\rho D K_T}{c_s}\left(\frac{\partial^2 C}{\partial \bar{x}^2} + \frac{\partial^2 C}{\partial \bar{y}^2}\right) \end{aligned} \tag{13}$$

$$\left(\bar{u}\frac{\partial}{\partial \bar{x}} + v\frac{\partial}{\partial \bar{y}}\right)C = D\left(\frac{\partial^2 C}{\partial \bar{x}^2} + \frac{\partial^2 C}{\partial \bar{y}^2}\right) + \frac{DK_T}{T_m}\left(\frac{\partial^2 T}{\partial \bar{x}^2} + \frac{\partial^2 T}{\partial \bar{y}^2}\right) \tag{14}$$

The non-dimensional quantities

$$x=\frac{\overline{x}}{\lambda},\ y=\frac{\overline{y}}{d_1},\ u=\frac{\overline{u}}{c},\ v=\frac{\overline{v}}{c\delta},\ p=\frac{d_1^2}{c\mu\lambda}\overline{p},\ h_1=\frac{h_1}{d_1},\ h_2=\frac{h_2}{d_1},\overline{k}=\frac{\beta}{d_1^{\,2}}$$

$$\delta=\frac{d_1}{\lambda},\ \eta=\frac{\eta^*}{\mu d_1^2},\ R_e=\frac{\rho c d_1}{\mu},\ Fr=\frac{c^2}{g d_1},\ k=\frac{k_0 c}{\mu d_1},\ \Phi=\frac{d_1^2}{\mu c^2}\overline{\Phi}$$

$$\gamma=\frac{T-T_0}{T_1-T_0},\ Ec=\frac{c^2}{\xi\left(T_1-T_0\right)},\ \Pr=\frac{\xi\mu}{k},\ \varphi=\frac{C-C_0}{C_1-C_0},\ Sc=\frac{\mu}{\rho D},$$

$$Sr=\frac{\rho D K_T\left(C_1-C_0\right)}{\mu T_m\left(T_1-T_0\right)},\ Du=\frac{\rho D K_T\left(C_1-C_0\right)}{\mu\xi c_s\left(T_1-T_0\right)},\ M^2=\frac{\sigma^* B_0^2 d_1^2}{\mu},\ Br=\Pr Ec. \tag{15}$$

Equations (10) – (14) take the form

$$\frac{\partial u}{\partial x}+\frac{\partial v}{\partial y}=0, \tag{16}$$

$$\delta\,\mathrm{Re}\left(u\frac{\partial}{\partial x}+v\frac{\partial}{\partial y}\right)u=-\frac{\partial p}{\partial x}+\delta^2\frac{\partial^2 u}{\partial x^2}+\frac{\partial^2 u}{\partial y^2}-\eta\left(\delta^4\frac{\partial^4 u}{\partial x^4}+2\delta^2\frac{\partial^4 u}{\partial x^2\partial y^2}+\frac{\partial^4 u}{\partial y^4}\right)$$
$$-\frac{M^2}{1+m^2}\cos\theta\left(u\cos\theta-v\delta\sin\theta+\cos\theta\right)+\frac{\mathrm{Re}}{Fr}\sin\alpha \tag{17}$$

$$\delta^3\,\mathrm{Re}\left(u\frac{\partial}{\partial x}+v\frac{\partial}{\partial y}\right)v=-\frac{\partial p}{\partial y}+\delta^2\left(\delta^2\frac{\partial^2 v}{\partial x^2}+\frac{\partial^2 v}{\partial y^2}\right)-\eta\delta^2\left(\delta^4\frac{\partial^4 v}{\partial x^4}+2\delta^2\frac{\partial^4 v}{\partial x^2\partial y^2}+\frac{\partial^4 v}{\partial y^4}\right)$$
$$+\frac{M^2}{1+m^2}\delta\sin\theta\left(u\cos\theta-v\delta\sin\theta+\cos\theta\right)-\delta\frac{\mathrm{Re}}{Fr}\cos\alpha \tag{18}$$

$$\delta\,\mathrm{Re}\Pr\left(u\frac{\partial}{\partial x}+v\frac{\partial}{\partial y}\right)\gamma=\delta^2\frac{\partial^2\gamma}{\partial x^2}+\frac{\partial^2\gamma}{\partial y^2}+Br\left[2\delta^2\left(\frac{\partial u}{\partial x}\right)^2+2\delta^2\left(\frac{\partial v}{\partial y}\right)^2\times\left(\frac{\partial u}{\partial y}+\delta^2\frac{\partial v}{\partial x}\right)^2\right]$$
$$+\eta Br\left[\delta^2\left(\delta^2\frac{\partial^2 v}{\partial x^2}+\frac{\partial^2 v}{\partial y^2}\right)^2+\left(\delta^2\frac{\partial^2 u}{\partial x^2}+\frac{\partial^2 u}{\partial y^2}\right)^2\right]$$
$$+\Pr Du\left(\delta^2\frac{\partial^2\varphi}{\partial x^2}+\frac{\partial^2\varphi}{\partial y^2}\right) \tag{19}$$

$$\delta\,\mathrm{Re}\left(u\frac{\partial}{\partial x}+v\frac{\partial}{\partial y}\right)\varphi=\frac{1}{Sc}\left(\delta^2\frac{\partial^2\varphi}{\partial x^2}+\frac{\partial^2\varphi}{\partial y^2}\right)+Sr\left(\delta^2\frac{\partial^2\gamma}{\partial x^2}+\frac{\partial^2\gamma}{\partial y^2}\right), \tag{20}$$

where Re is the Reynolds number, Fr is the Froude number, Pr is the Prandtl number. Br is the Brinkman number, Du is the Dufour number, Sc is the Schmidt number and Sr is the Soret number, β is the permeable parameter.

The assumptions of long wave length $(\delta << 1)$ and low Reynolds number $(\mathrm{Re}\to 0)$

Equations (17) – (20) gives

$$-\frac{\partial p}{\partial x}+\frac{\partial^2 u}{\partial y^2}-\eta\frac{\partial^4 u}{\partial y^4}-\frac{M^2}{1+m^2}\cos\theta\left(u\cos\theta+\cos\theta\right)+\frac{\mathrm{Re}}{Fr}\sin\alpha=0 \tag{21}$$

$$\frac{\partial^2 \gamma}{\partial y^2} + Br\left(\frac{\partial u}{\partial y}\right)^2 + \eta Br\left(\frac{\partial^2 u}{\partial y^2}\right)^2 + \Pr Du\frac{\partial^2 \varphi}{\partial y^2} = 0, \tag{22}$$

$$\frac{\partial^2 \varphi}{\partial y^2} + ScSr\frac{\partial^2 \gamma}{\partial y^2} = 0, \tag{23}$$

In which incompressibility condition is automatically satisfied and Eq. (20) shows that $p \neq p(y)$.

The corresponding boundary conditions and wall geometries $h_1(x)$ and $h_2(x)$ in the dimensionless form are

$$u = -1 - \frac{1}{\beta\sigma}\frac{\partial u}{\partial y}, \quad \frac{\partial^2 u}{\partial y^2} = 0, \quad \gamma = 0, \quad \varphi = 0, \quad at \;\; y = h_1 = 1 + a\sin(2\pi x), \tag{24}$$

$$u = -1 + \frac{1}{\beta\sigma}\frac{\partial u}{\partial y}, \quad \frac{\partial^2 u}{\partial y^2} = 0, \quad \gamma = 1, \quad \varphi = 1, \quad at \;\; y = h_2 = -d - b\sin(2\pi x + \phi), \tag{25}$$

Where $a = a_1 / d_1,\;\; b = a_2 / d_1 \;\; and \;\; d = d_2 / d_1$ satisfy the condition

$$a^2 + b^2 + 2ab\cos\phi \leq (1+d)^2. \tag{26}$$

The dimensionless average flux F in the wave frame is

$$F = \int_{h_2}^{h_1} u dy. \tag{27}$$

The above flux in the laboratory frame σ is related to

$$\sigma = F + 1 + d. \tag{28}$$

The non-dimensional expression for the pressure rise per wavelength Δp_λ is defined by

$$\Delta p_\lambda = \int_0^1 \left(\frac{dp}{dx}\right) dx. \tag{29}$$

Solutions of the problem

The closed form solution of Eq. (21) is

$$u(y) = C_1 e^{yM_1} + C_2 e^{-yM_1} + C_3 e^{yM_2} + C_4 e^{-yM_2} - \frac{H}{z}, \tag{30}$$

Where $z = \frac{M^2}{1+m^2}\cos^2\theta, \quad H = \frac{dp}{dx} + z - \frac{\mathrm{Re}}{Fr}\sin\alpha + \frac{\mu}{\beta}$ (31)

Now result for $\frac{dp}{dx}$ can be easily evaluated using Eqs. (27), (30) and (31) .Substituting Eqs. (30), (31) and (23) into Eq. (22) to get the closed form solution of $\gamma(y)$:

$$\gamma = C_5 + C_6 y + \frac{Br}{-1+\Pr DuScSr}\left[\begin{array}{l}\frac{1}{4}C_1^2\left(1+\eta M_1^2\right)e^{2M_1 y}+\frac{1}{4}C_2^2\left(1+\eta M_1^2\right)e^{-2M_1 y}+\frac{1}{4}C_3^2\left(1+\eta M_2^2\right)e^{2M_2 y}\\ +\frac{1}{4}C_4^2\left(1+\eta M_2^2\right)e^{-2M_2 y}+2M_1M_2C_1C_3\left(1+\eta M_1M_2\right)\frac{e^{(M_1+M_2)y}}{\left(M_1+M_2\right)^2}\\ +2M_1M_2C_1C_4\left(-1+\eta M_1M_2\right)\frac{e^{(M_1-M_2)y}}{\left(M_1-M_2\right)^2}\\ +2M_1M_2C_2C_3\left(-1+\eta M_1M_2\right)\frac{e^{-(M_1-M_2)y}}{\left(M_1-M_2\right)^2}\\ +2M_1M_2C_2C_4\left(1+\eta M_1M_2\right)\frac{e^{-(M_1+M_2)y}}{\left(M_1+M_2\right)^2}\\ +M_1^2C_1C_2\left(-1+\eta M_1^2\right)y^2+M_2^2C_3C_4\left(-1+\eta M_2^2\right)y^2\end{array}\right] \quad (32)$$

By solving Eq. (23) we get the closed form solution of ϕ as follows:

$$\varphi = C_7 + C_8 y - \frac{ScSrBr}{-1+\Pr DuScSr}\left[\begin{array}{l}\frac{1}{4}C_1^2\left(1+\eta M_1^2\right)e^{2M_1 y}+\frac{1}{4}C_2^2\left(1+\eta M_1^2\right)e^{-2M_1 y}+\frac{1}{4}C_3^2\left(1+\eta M_2^2\right)e^{2M_2 y}\\ +\frac{1}{4}C_4^2\left(1+\eta M_2^2\right)e^{-2M_2 y}+2M_1M_2C_1C_3\left(1+\eta M_1M_2\right)\frac{e^{(M_1+M_2)y}}{\left(M_1+M_2\right)^2}\\ +2M_1M_2C_1C_4\left(-1+\eta M_1M_2\right)\frac{e^{(M_1-M_2)y}}{\left(M_1-M_2\right)^2}\\ +2M_1M_2C_2C_3\left(-1+\eta M_1M_2\right)\frac{e^{-(M_1-M_2)y}}{\left(M_1-M_2\right)^2}\\ +2M_1M_2C_2C_4\left(1+\eta M_1M_2\right)\frac{e^{-(M_1+M_2)y}}{\left(M_1+M_2\right)^2}\\ +M_1^2C_1C_2\left(-1+\eta M_1^2\right)y^2+M_2^2C_3C_4\left(-1+\eta M_2^2\right)y^2\end{array}\right] \quad (33)$$

where $M_1 = \sqrt{-\frac{-1+\sqrt{1-4\eta z}}{2\eta}}$ and $M_2 = \sqrt{\frac{-1+\sqrt{1-4\eta z}}{2\eta}}$ (34)

And the constants $c_i (i = 1-8)$ in Equations (30),(32) and (33) can be calculated by simple algebraic computations.

3. GRAPHICAL RESULTS AND DISCUSSION

Pumping characteristics

This section addresses the nature of longitudinal pressure gradient dp/dx and pressure rise per wavelength Δp_λ for different flow parameters involved in this problem. The equation (29) involves the integration of dp/dx but this integral is not solvable by analytically. So we computed it numerically by the tool "Mathematical". The pressure gradient for different values of couple stress parameter η against x is plotted in Figure 2. It is observed that dp/dx increases in the narrow part of the channel while it decreases in the major part of the channel. Figure 3 indicates the effect of Hall parameter m on dp/dx. It shows that dp/dx decreases in the narrow part of the channel and it increases in the major part. Figure 4 represents that larger Hartmann number M decrease dp/dx in major part of the channel while dp/dx increases at the narrow part of the channel. Figure 5 reveals that dp/dx increases

when angle of inclination α increases. The pressure gradient for different values of permeability parameter β against x is plotted in Figure 6. It depicts that dp/dx increases in the narrow part of the channel while it decreases in the major part of the channel.

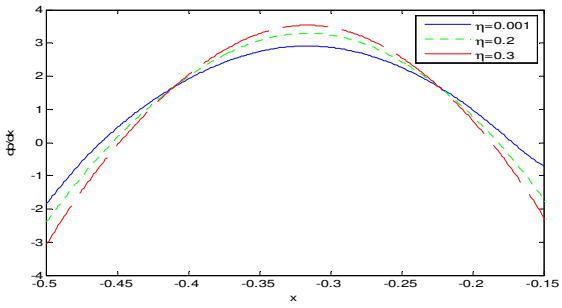

Figure 2 Variation of pressure gradient dp/dx for different values of η with $a=0.6$, b=0.7, d=1.5, R = 0.5, $\phi=\pi/4$, m=0.03, M=4, $\alpha=\frac{\pi}{3},\theta=\frac{\pi}{3},Fr=1.2,\sigma=1,\beta=0.1.$

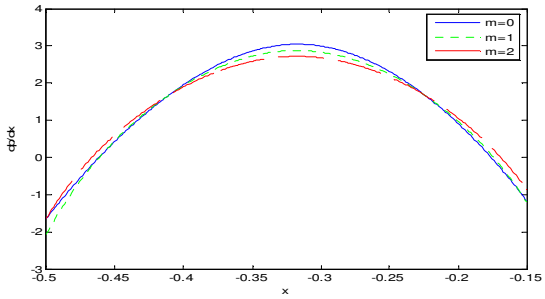

Figure 3 Variation of pressure gradient dp/dx for different values of m with $a=0.6$, b=0.7, d=1.5, R = 0.5, $\phi=\pi/4$, $\eta=0.1$, M=4, $\alpha=\frac{\pi}{3},\theta=\frac{\pi}{3},Fr=1.2,\sigma=1,\beta=0.1.$

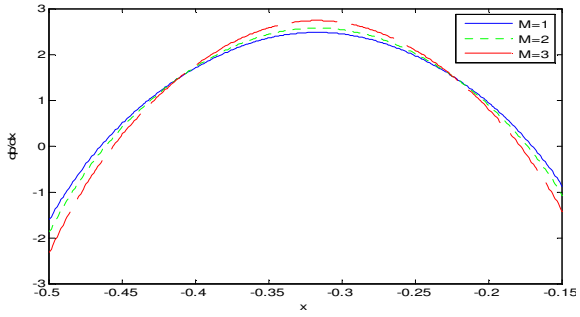

Figure 4 Variation of pressure gradient dp/dx for different values of M with $a=0.6$, b=0.7, d=1.5, R=0.5, $\phi=\pi/4$, $\eta=0.1$, m=0.03, $\alpha=\frac{\pi}{3},\theta=\frac{\pi}{3},Fr=1.2,\sigma=1,\beta=0.1.$

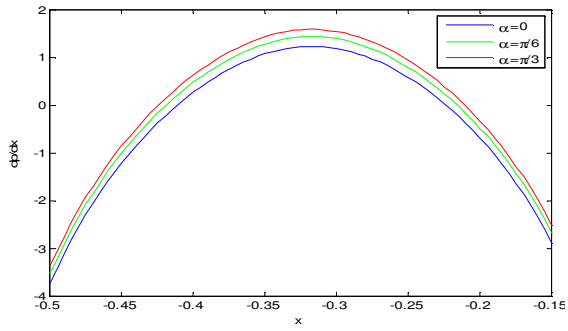

Figure 5 Variation of pressure gradient dp/dx for different values of α with $a=0.6$, b=0.7, d=1.5, R = 0.5, $\eta=0.1$, M=4, m=0.03, $\phi=\frac{\pi}{4},\theta=\frac{\pi}{3},Fr=1.2,\sigma=1,\beta=0.1.$

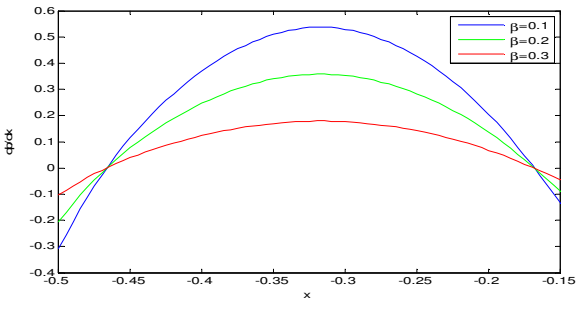

Figure 6 Variation of pressure gradient dp/dx for different values of β with $a=0.6$, b=0.7, d=1.5, R = 0.5, $\eta=0.1$, M=4, m=0.03, $\alpha=\frac{\pi}{3},\theta=\frac{\pi}{3},Fr=1.2,\sigma=1,\phi=\frac{\pi}{4}.$

Figure 7-10 represents the variation of the pressure rise per wavelength Δp_λ versus average flux σ. From Figure 7 we noted that in peristaltic pumping region $(\Delta p_\lambda > 0, \sigma > 0)$ the pressure rise increases where as it decreases in the co pumping region $(\Delta p_\lambda < 0,\ \sigma > 0)$ with an increase in the couple stress parameter η. This shows that the peristaltic pumping for the non-Newtonian fluid $(\eta \neq 0)$ is greater in comparison to the Newtonian fluid $(\eta \to 0)$. In Figure 8, the variation of pressure rise Δp_λ with the increasing value of Hartman number M is shown. We found that pressure rise Δp_λ increases in the peristaltic pumping region $(\Delta p_\lambda > 0, \sigma > 0)$ while it decreases in the co pumping region $(\Delta p_\lambda < 0, \sigma > 0)$. In Figure 9 observed that the pressure rise decreases in the retrograde region $(\Delta p_\lambda > 0, \sigma < 0)$ and it increases in the co pumping region $(\Delta p_\lambda < 0, \sigma > 0)$ when the Hall parameter m increases. Figure 10 indicates that the pressure rise decreases for increasing values of permeability parameter β in the pumping and co-pumping region.

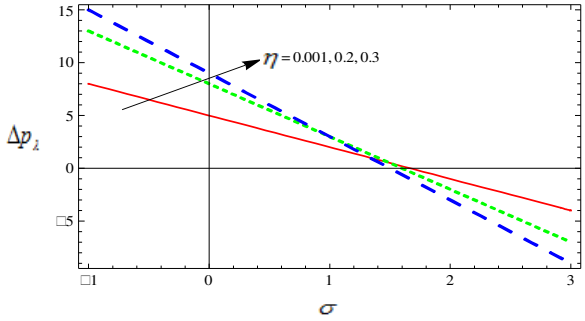

Figure 7 Variation of pressure rise Δp_λ for different values of η with $a = 0.7$, b=1.2, d=2, R=0.5, Fr=1.2, $\phi = \pi/4$, m= 0.03, M=4, $\theta = \pi/3$, $\alpha = \frac{\pi}{3}, \beta = 0.1$.

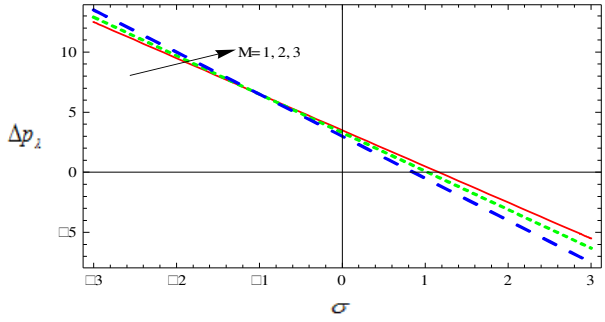

Figure 8 Variation of pressure rise Δp_λ for different values of M with $a = 0.7$, b=1.2, d=2, R=0.5, $\eta = 0.1$, $\phi = \pi/4$, m= 0.03, Fr=1.2, $\theta = \pi/3$, $\alpha = \frac{\pi}{3}, \beta = 0.1$.

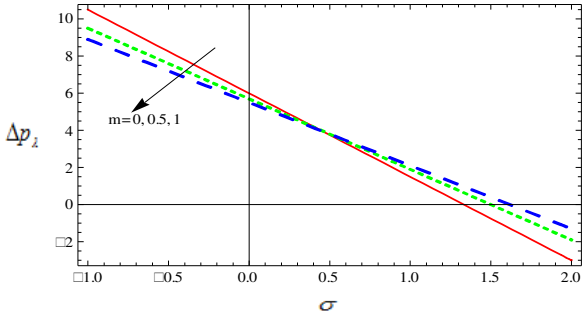

Figure 9 Variation of pressure rise Δp_λ for different values of m with $a = 0.7$, b=1.2, d=2, R=0.5, $\eta = 0.1$, $\phi = \pi/4$, M= 4, Fr=1.2, $\theta = \pi/3$, $\alpha = \frac{\pi}{3}, \beta = 0.1$.

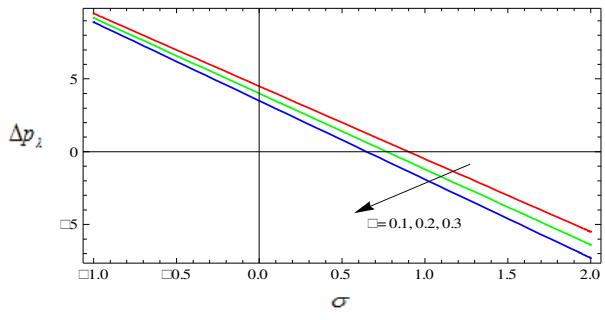

Figure 10 Variation of pressure rise Δp_λ for different values of β with $a = 0.7$, b=1.2, d=2, R=0.5, $\eta = 0.1$, $\theta = \pi/3$, M= 4, Fr=1.2,m=0.03, $\alpha = \frac{\pi}{3}, \phi = \frac{\pi}{4}$.

Velocity behavior

In this section the effects of various physical parameters on the velocity profile $u(y)$ are analyzed. Figure 11 depicts that magnitude of the velocity profile $u(y)$ decreases as couple stress parameter η increases. Figures 12 and 13 reveals that decreases the velocity profile $u(y)$ with the increase of Hartmann number M whereas it increases with the increase of Hall parameter m. Figure 14 indicates that the velocity profile $u(y)$ increases for increasing angle of inclination α and in figure 15 we observed that the velocity profile $u(y)$ decreases with the increase of permeability parameter β.

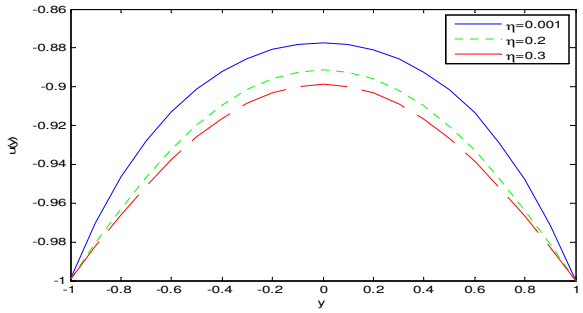

Figure 11 Variation of velocity field $u(y)$ for different values of η with $a=0.6$, b=0.7, d=1.5, R=2, $\sigma=1$, M=4,m=0.03,x=-0.5, $\phi=\pi/4$, $dp/dx=1$, $Fr=1.2, \alpha=\frac{\pi}{3}, \theta=\frac{\pi}{3}, \beta=0.1$.

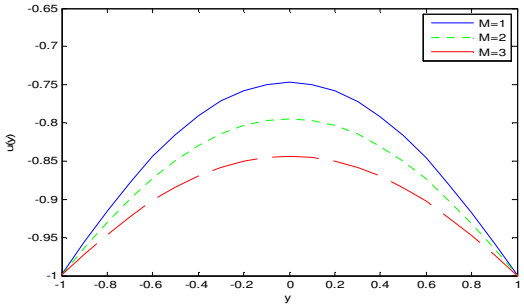

Figure 12 Variation of velocity field $u(y)$ for different values of M with $a=0.6$, b=0.7, d=1.5, R=2, $\eta=0.1$, $\sigma=1$, m=0.03, x=-0.5, $\phi=\pi/4$, $dp/dx=1$, $Fr=1.2, \alpha=\frac{\pi}{3}, \theta=\frac{\pi}{3}, \beta=0.1$.

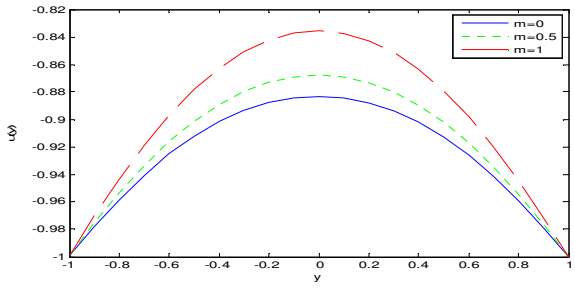

Figure 13 Variation of velocity field $u(y)$ for different values of m with $a=0.6$, b=0.7, d=1.5, R=2, $\eta=0.1$, $\sigma=1$,M=4,x=-0.5, $\phi=\pi/4$, $dp/dx=1$, $Fr=1.2, \alpha=\frac{\pi}{3}, \theta=\frac{\pi}{3}, \beta=0.1$.

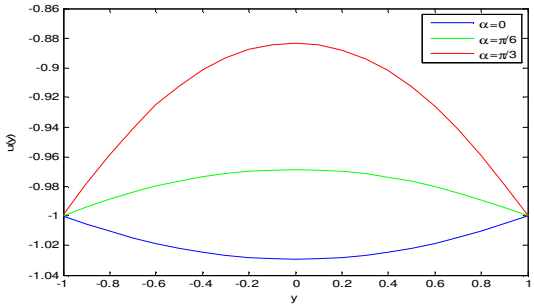

Figure 14 Variation of velocity field $u(y)$ for different values of α with $a=0.6$, b=0.7, d=1.5, R=2, $\eta=0.1$, $\sigma=1$, m=0.03,M=4,x=-0.5, $\phi=\pi/4$, $dp/dx=1$, $Fr=1.2, \theta=\frac{\pi}{3}, \beta=0.1$.

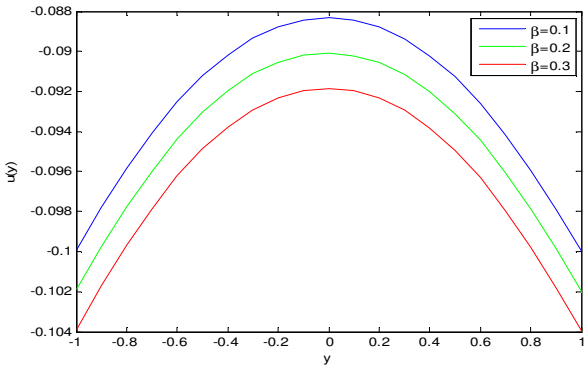

Figure 15 Variation of velocity field $u(y)$ for different values of β with $a=0.6$, b=0.7, d=1.5, R=2, $\eta=0.1$, $\sigma=1$, m=0.03, M=4, x=-0.5, $\phi=\pi/4$, $dp/dx=1$, $Fr=1.2$, $\theta=\frac{\pi}{3}$, $\alpha=\frac{\pi}{3}$.

Temperature profile

Figures 16-20 display the variations in the temperature profile $\gamma(y)$ for several values of parameters of interest. In Figure 16, we observed that the temperature profile $\gamma(y)$ decreases as couple stress parameter η increases. As per Figure 17, the temperature profile $\gamma(y)$ and Hartmann number M are in inversely proportional. Figures 18 shows that with an increase of Hall parameter m, the temperature profile $\gamma(y)$ increases. Figure 19 and 20 illustrates that the temperature profile $\gamma(y)$ decreases with the increase of angle of inclination α whereas it increases with the increase of permeability parameter β.

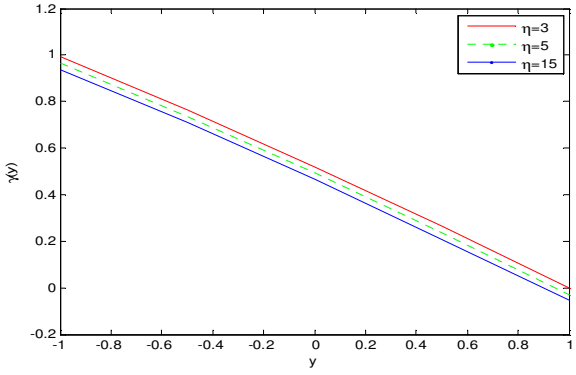

Figure 16 Variation of temperature profile $\gamma(y)$ for different values of η with $a=0.6$, b=0.7, d=1.5, R=0.5, M=4, Fr=1.2, m=0.03, x=-0.5, Du=0.1, Sc=0.5, Br=Pr=2, Sr=0.6 $\sigma=1$, $\phi=\pi/4$, $\theta=\pi/3$, $dp/dx=1$, $\alpha=\frac{\pi}{3}$, $\beta=0.1$.

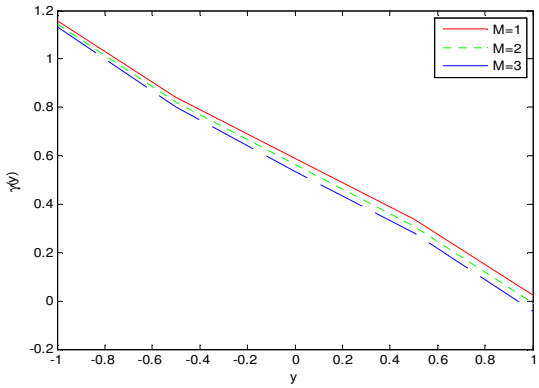

Figure 17 Variation of temperature profile $\gamma(y)$ for different values of M with $a=0.6$, b=0.7, d=1.5, R=0.5, $\eta=0.1$, Fr=1.2, m=0.03, x=-0.5, Du=0.1, Sc=0.5, Br=Pr=2, Sr=0.6 $\sigma=1$, $\phi=\pi/4$, $\theta=\pi/3$, $dp/dx=1$, $\alpha=\frac{\pi}{3}$, $\beta=0.1$.

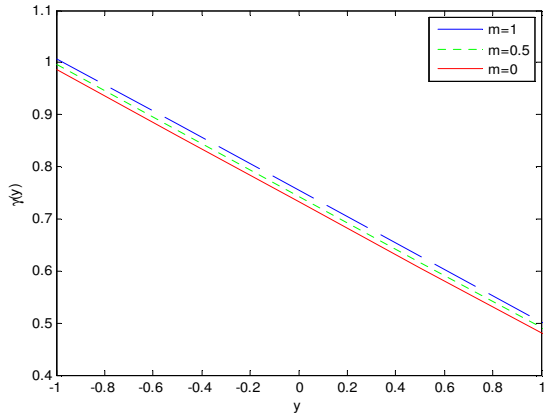

Figure 18 Variation of temperature profile $\gamma(y)$ for different values of m with $a=0.6$, b=0.7, d=1.5, R=0.5, $\eta=0.1$, Fr=1.2, $\theta=\pi/3$, x=-0.5, Du=0.1, Sc=0.5, Br=Pr=2, Sr=0.6 $\sigma=1, \phi=\pi/4$, M=4, $dp/dx=1$, $\alpha=\frac{\pi}{3}, \beta=0.1$.

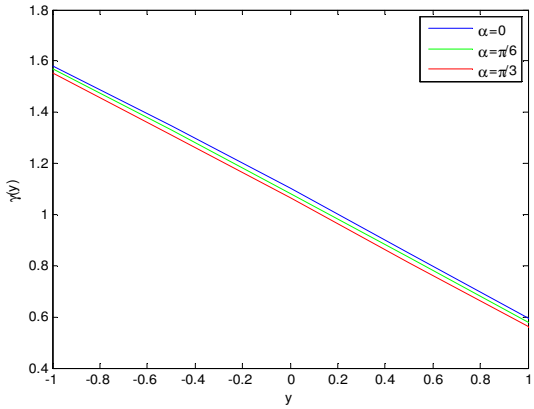

Figure 19 Variation of temperature profile $\gamma(y)$ for different values of α with $a=0.6$, b=0.7, d=1.5, R=0.5, $\eta=0.1$, m=0.03, $\theta=\pi/3$, x=-0.5, Du=0.1, Sc=0.5, Br=Pr=2, Sr=0.6, $\sigma=1$, $\phi=\pi/4$, $dp/dx=1$, M=4, , $Fr=1.2, \beta=0.1$.

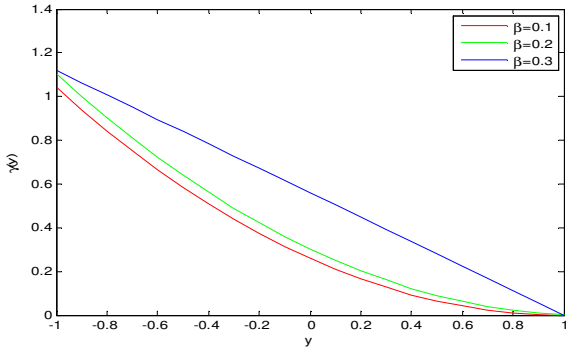

Figure 20 Variation of temperature profile $\gamma(y)$ for different values of β with $a=0.6$, b=0.7, d=1.5, R=0.5, $\eta=0.1$, m=0.03, $\theta=\pi/3$ x=0.5, Du=0.1, Sc=0.5, Br=Pr=2, Sr=0.6 $\sigma=1, \phi=\pi/4$, M=4, $dp/dx=1$, $Fr=1.2, \alpha=\frac{\pi}{3}$.

Concentration profile

Here we plot the figures between the concentration profile $\phi(y)$ and various values of physical parameters and determines the performance of concentration profile $\phi(y)$. As per Figure 21, $\phi(y)$ is directly proportional to η. In couple stress fluid $(\eta \neq 0)$ the concentration profile $\phi(y)$ is strengthened when compared to couple stress fluids $(\eta \to 0)$. Figure22 reveals that concentration profile $\phi(y)$ increases with the increase of Hartmann number M due to decrease of the velocity. Figure 23 depicts that the concentration profile $\phi(y)$ decreases with the increasing of Hall parameter m. In Figure 24 we observed that the concentration profile $\phi(y)$ increases with the increasing of permeability parameter β.

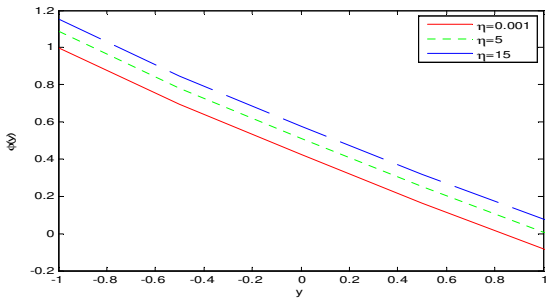

Figure 21 Variation of concentration profile $\phi(y)$ for various values of η with $a=0.6$, b=0.7, d=1.5, R=0.2, M=2, Fr=1.2, m=0.03, x=-0.5, Du=0.1, Sc=1, Br=2, Pr=4,Sr=0.6 $\sigma=1, \phi=\pi/4$, $\theta=\pi/3$, $dp/dx=2$, $\alpha=\frac{\pi}{3}, \beta=0.1$.

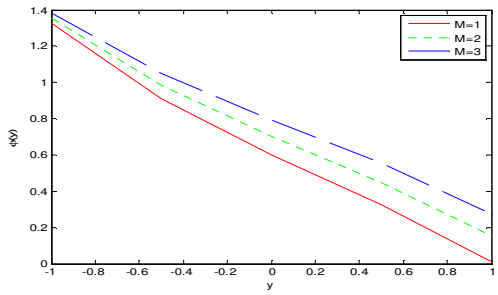

Figure 22 Variation of temperature profile $\phi(y)$ for different values of M with $a=0.6$, b=0.7, d=1.5, R=0.2, $\eta=0.1$, Fr=1.2, m=0.03, x=-0.5, Du=0.1, Sc=1, Br=2, Pr=4, Sr=0.6 $\sigma=1, \phi=\pi/4, \theta=\pi/3$, $dp/dx=2$, $\alpha=\frac{\pi}{3}, \beta=0.1$.

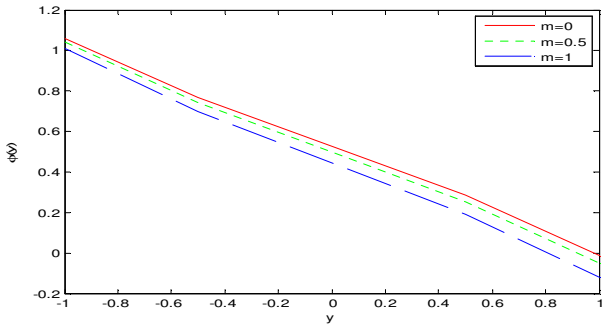

Figure 23 Variation of concentration profile $\phi(y)$ for different values of m with $a=0.6$, b=0.7, d=1.5, R=0.2, M=2, $\eta=0.1$, Fr=1.2, x=-0.5, Du=0.1, Sc=1, Br=2, Pr=4, Sr=0.6 $\sigma=1, \phi=\pi/4, \theta=\pi/3$, $dp/dx=2$, $\alpha=\frac{\pi}{3}, \beta=0.1$.

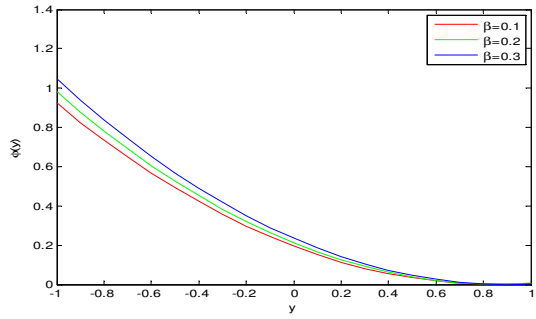

Figure 24 Variation of concentration profile $\phi(y)$ for different values of β with $a=0.6$, b=0.7, d=1.5, R=0.2, M=2, $\eta=0.1$, Fr=1.2, x=-0.5, Du=0.1, Sc=1, Br=2, Pr=4, Sr=0.6 $\sigma=1, \phi=\pi/4$,m=0.03, $dp/dx=2$, $\theta=\pi/3$, $\alpha=\frac{\pi}{3}$.

4. CONCLUSIONS

The peristaltic flow of a couple stress fluid in an inclined asymmetric channel with permeable walls is investigated. Hall effects are taken into account. The main findings are mentioned below.

- The pressure gradient dp/dx increases in the narrow part of the channel and it decreases in the major part of the channel with the increasing of couple stress parameter η and permeability parameter β.
- The pressure rise Δp_λ decreases in the retrograde region and it increases in the co pumping region when the Hall parameter m increases. Pressure rise Δp_λ decreases in all pumping regions when permeability parameter β increases.
- With an increase of Hall parameter m, the magnitude of velocity profile $u(y)$ increases.

- Variation of permeability parameter β opposite behavior when compared with m.
- The temperature profile $\gamma(y)$increases for increasing values of Hall parameter m and permeability parameter β .
- Concentration Profile $\phi(y)$is a decreasing function of m and decreasing function of β .

REFERENCES

[1] T. W. Latham, Fluid motion in a peristaltic pump, M.sc. thesis, MIT, Cambridge, MA (1966).

[2] A. H. Shapiro, M. Y. Jaffrin and S.L. Weinberg, Peristaltic pumping with long Wavelengths at low Reynolds number, J. Fluid Mech. 37 (1969) 799-825.

[3] Stokes VK, Couple Stresses in Fluids, Phys Fluids 9:1709-1715, 1966.

[4] Srivastava LM, Peristaltic transport of a couple-stress fluid, Rheol Acta 25:638-641, 1986.

[5] Zueco J, Beg OA, Network numerical simulation applied to pulsatile non-Newtonian flow through a channel with couple stress and wall mass flux effects, Int J Appl Math Mech5(2):1-16, 2009.

[6] Ghosh SK, Beg OA, Bhargava R, Rawat S, Beg TA, Mathematical modelling of transient magnetohydrodynamic couple stress fluid flow in a rotating channel, Int J Appl Math Mech 6(6):23-45, 2010.

[7] Valanis KC, Sun CT, Poiseuille Flow of Fluid with Couple Stress with Applications to Blood Flow, Biorheology 6(2):85-97, 1969.

[8] Popel AS, Regirer SA, Usick PI, A Continuum Model of Blood Flow, Biorheology 11:427-437, 1974.

[9] Shehawey EFE, Mekheimer KS, Couple stresses in peristaltic transport of fluids, J Phys D: Appl Phys 27:1163-1170, 1994.

[10] S. C. Cowin, The theory of polar fluids, Adv. Appl. Mech. 14 (1974) 279-347.

[11] A.Beg, J.Zueco and T.B.Chang, Numerical analysis of hydromagnetic gravity-driven Thin film micropolar flow along an included plane, Chem. Engrg. Common. 198 (2011) 312-331.

[12] N.Ali and T.Hayat, Peristaltic flow of a micropolar fluid in an asymmetric channel, Comp. Math. Appl. 55 (2008) 589-608.

[13] T.Hayat, N. Ali and S,Asghar, Hall effects on peristaltic flow of a Maxwell fluid in a Porous medium, Phys. Lett. A 363 (2007) 397-403.

[14] S. Srinivas and R. Gayathri, Peristaltic transport of a Newtonian fluid in a vertical Asymmetric channel with heat transfer and porous medium, Applied Mathematics and Computation Volume 215, Issue 1, 1 September 2009, Pages 185–196.

[15] S. Nadeem and Noreen Sher Akbar, Influence of heat and mass transfer on the peristaltic Flow of a Johnson Segalman fluid in a vertical asymmetric channel with induced MHD, Journal of the Taiwan Institute of Chemical Engineers, Volume 42, Issue 1, January 2011,Pages 58–66.

[16] A.Kavitha, R. Hemadri Reddy, S. Sreenadh, R. Saravana and A. N. S. Srinivas, Peristaltic Flow of a micro polarfluid in a vertical channel with longwave length approximation, Pelagia Research Library Advances in Applied Science Research, 2011, 2 (1): 269-279.

[17] K. Vajravelu, S. Sreenadh and P. Lakshminarayana, The influence of heat transfer on Peristaltic transport of a Jeffrey fluid in a vertical porous stratum, Simulation, Volume, August 2011, Pages 3107–3125.

[18] G. Rami Reddy and S. Venkataramana, Peristaltic transport of a conducting fluid through a porous medium in an asymmetric vertical channel, Pelagia Research Library Advances in Applied Science Research, 2011, 2 (5):240-248.

[19] N.S. Gad, Effect of Hall currents on interaction of pulsatile and peristaltic transport Induced flows of a particle-fluid suspension, Appl. Math. Comput. 217 (2011) 4313-4320.

[20] E. Abo-Eldahab, E. Barakart and Kh. Nowar, Hall currents and heat transfer effects on Peristaltic transport in a vertical asymmetric channel through a porous medium, Math. Probl. Engrg. 2012 (2012) 840203

[21] A.Govindarajn, E.P Siva, M.Vidhya , Combined effect of heat and mass transfer on MHD Peristaltic transport of a couple stress fluid in a inclined asymmetric channel through Porous medium, IJPAM-volume-105, No.4, 2015, 685-707.

[22] J.Srinivas and J.V. Ramana Murthy, flow of two immiscible couple stress fluids between two permeable beds, Journal of Applied Fluid Mechanics, Vol. 9, No. 1, pp. 501-507, 2016.

[23] T.Hayat, Maryam Iqbal, Humaira Yasmin and Faud Alsaadi, Hall effects on peristaltic Flow of couple stress fluid in an inclined asymmetric channel, International Journal of Biomathematics, Vol. 7, No.5 (2014) 1450057 (34 pages)

[24] J.Suresh Goud and R.Hemadri Reddy, Peristaltic Transport of a Pseudoplastic Fluid Bounded By Permeable Walls with Suction and Injection, International Journal of Pure and Applied mathematics, Vol. 113, No.6 (2017), 289-297

[25] J.Suresh Goud and R.Hemadri Reddy, A Review Chronicle of Recent Trends In Peristaltic Transport of Non-newtonian Fluids, International Journal of pharmacy and technology, Vol. 8, No.4 (2016), 5118-5131

[26] J.Suresh Goud,R.Hemadri Reddy and R Saravana Peristaltic Transport of a Bingham Fluid in Contact with a Newtonian Fluid in a Vertical Channel IOP Conf. Series: Materials Science and Engineering 263 (2017) 062005 doi:10.1088/1757-899X/263/6/062005.

[27] R Saravana, R.Hemadri Reddy and J.Suresh Goud MHD peristaltic flow of a hyperboli tangent fluid in a non-uniform channel with heat and mass transfer IOP Conf. Series: Materials Science and Engineering 263 (2017) 062006 doi:10.1088/1757-899X/263/6/062006.

[28] J.Suresh Goud and R.Hemadri Reddy Effects Of Slip On Peristaltic Flow Of A Rabinowitsch Fluid Model In A Uniform Tube Journal of Advanced Research in Dynamical and Control Systems Vol. 9, Issue 3, Nov.2017

Mr. J Suresh Goud is a Reaseach scholar in Mathematics under the fluid dynamics division in VIT University vellore, Tamilnadu. Now, Mr Goud is working as Assistant professor in the department of mathematics **at Institute of Aeronautical Engineering, An autonomous engineering college at Hyderabad**. He has published 6 scopus indexed journals in his thrust area of research -fluid dynamics.

Dr R Hemadri Reddy is working as a Senior Assistant professor of Mathematics under the fluid dynamics division in VIT University vellore, Tamilnadu since 2010. Dr Reddy has published 30 international journals including 20 Scopus indexed journals in fluid dynamics. His thrust areas of research include PDE, ODE, Fluid Dynamics.